DOI: 10.24996/ijs.2026.67.6.7

ISSN: 0067-2904

Preparation and characterization the microstructure and the surface area of magnesium oxide nanoparticles

Shaimaa A. Jadoo, Wedad J. Fendi, Juman A. Naser, Jasim M. S. Jamur*
Department of Chemistry, College of Education for Pure Science (Ibn Al- Haitham), University of Baghdad, Iraq.

Received: 22/10/2024 Accepted: 24/7/2025 Published: 30/6/2026

Abstract

Magnesium oxide nanoparticles were synthesized via a co-precipitation procedure. Comprehensive characterization included infrared fluorescence, X-ray scattering spectroscopy, scanning electron microscopy, as well as X-ray diffraction and atomic force microscopy. Surface properties were analyzed using Langmuir, Brunauer -Emmett-Teller, Barrett–Joyner–Halenda, t-plot techniques, and the N_2 adsorption-desorption isotherms methods to determine surface area and pore structure. Results confirmed the nanoparticles possess high purity. The size of the synthesized particles ranged from 30-40 nm, which was determined by scanning electron microscopy. The surface area of the prepared particles is 31,227 m^2 g^{-1}, and it was found that the pore volume was 0.03031 cm3 m^{-1}, while the pore diameter was 1.21 nm.

Keywords: magnesium oxide, pore diameter, nanoparticles, surface area, XRD, SEM.

تحضير وتشخيص البنية الدقيقة والمساحة السطحية لجسيمات اوكسيد المغنيسيوم النانوية

شيماء عبد الحسين جدوع، وداد جاسم فندي، جمان احمد ناصر، جاسم محمد شامار*
قسم الكيمياء، كلية التربية للعلوم الصرفة ابن الهيثم، جامعة بغداد، بغداد، العراق.

الخلاصة

تم تصنيع جسيمات نانوية من أوكسيد المغنيسيوم بتقنية الترسيب المشترك. شمل التوصيف الشامل فلورة الأشعة تحت الحمراء، وطيف تشتت الأشعة السينية، والمجهر الإلكتروني الماسح، بالإضافة إلى حيود الأشعة السينية ومجهر القوة الذرية. تم تحليل خصائص السطح باستخدام تقنيات لانكماير وبروناور–إيميت–تيلر، وباريت–جوينر–هاليندا، ومخطط t، وطرق تساوي درجة حرارة الامتزاز–الامتصاص لغاز النيتروجين (N2) لتحديد مساحة السطح وبنية المسام. أكدت النتائج نقاء الجسيمات النانوية العالي. تراوح حجم الجسيمات المُصنعة بين 30 و40 نانومتر، والذي تم تحديده باستخدام المجهر الإلكتروني الماسح. تبلغ مساحة سطح الجسيمات المُحضرة 31,227 م^2/غم، وتبين أن حجم المسام كان 0.03031 سم3/م، بينما بلغ قطر المسام 1.21 نانومتر.

*Email: jasim.m.s@ihcoedu.uobaghdad.edu.iq

1. Introduction

Nanomaterials, defined by their 1-100 nm size range, exhibit novel and distinctive qualities that set them apart from the materials from which they were produced [1,2]. Recent research has increasingly focused on nano-metal oxides due to their unique characteristics, including photocatalysis, hydrophobicity, stability, a large surface area, and reduced crystalline size [3,4]. Nanoscale metal oxides are also used in several applications such as coatings, batteries, catalysts, toxic waste treatment, capacitors, antibacterial agents, superconducting products, medical sciences, and sensors [5]. MgO NPs were prioritized for synthesis among metal oxides due to their unique qualities and properties, as they are characterized by their highly ionic nature, simple chemistry, and crystalline structure [6]. Nanoscale magnesium oxide is used in many applications such as photocatalysis [7], adsorption [8], foodborne antibacterials [9], ceramics, glass making [10], pharmaceuticals [11], catalysis, and optoelectronics [12].

Several synthesizing techniques have been employed, including laser ablation [13], the co-precipitation method [14], thermal reflux [15], and redox [16]. The co-precipitation method is used for its simplicity in terms of the raw materials used as well as ease of processing. The nanoparticles prepared by the co-precipitation method have a large surface area and small nano-sized sizes, which gives them a high adsorption capacity, so they are used in applications that require surface chemistry, including wastewater treatment [17,18].

Conventional methods of water purification result in hazardous waste and substances, necessitating energy-intensive processing [19]. This study aimed to synthesize MgO nanoparticles via the co-precipitation method, followed by characterization of the resulting particles using Fourier transform infrared spectroscopy (FTIR), atomic force microscopy (AFM), scanning electron microscopy (SEM), and X-ray diffraction (XRD). The model was also applied to the N_2 isotherms for adsorption-desorption, the specific surface area, and pore structure of the produced nanoparticles, as well as the Langmuir, Brunauer -Emmett-Teller (BET), Barrett-Joyner- Halenda (BJH), and t-plot techniques.

2. Materials and methods

2.1. Chemicals and reagents

Magnesium sulfate ($MgSO_4.7H_2O$) and ammonium hydroxide (NH_3OH) were supplied by the Sigma-Aldrich company.

2.2. Apparatus

The X-ray diffraction analysis was performed using a Shimadzu XRD-6000, while morphology was examined with a TESCAN S8000 Scanning electron microscope. FT-IR spectra were recorded on an IR Affinity 1800. Sample preparation utilized a LabTech hotplate magnetic stirrer, and measurements were conducted with a Sartorius electronic balance (model LMS-1003) and a CPA 22 device. The surface area analyzer was Belsorp MINI II ISO9277. All of these were produced by Shimadzu company.

2.3. Preparation of MgO NPs

MgO NPs were prepared using the co-precipitation method [20]. The magnesium sulfate ($MgSO_4.7H_2O$) aqueous solution (500 ml) was heated to 80 °C using a hotplate stirrer and used at a concentration of 0.02 M. Then, 400 ml of magnesium chloride solution with a concentration of 0.08M was gradually added while maintaining a steady temperature. A single addition of 20 ml (30%) ammonium hydroxide was then introduced while continuously stirring the mixture for 30 minutes. The precipitate was collected and repeatedly cleaned with distilled water until all traces of the base were removed once the mixture had reached room

temperature. Then the precipitate was heated to 500 °C for three hours to heat treat it (calcify it).

3. Results and discussion

3.1. FT-IR spectroscopy

The FTIR spectrum of the synthesized MgO NPs confirmed the formation of Mg-O bonds, indicated by absorption bands at 567 cm^{-1} and 879 cm^{-1} (Figure 1)[21], Furthermore, for the hydroxide group, the band appears as a bending vibration at 1419cm^{-1} uplink [22]. Additionally, the O-H group vibration in the water molecule causes a band to form at 3398 cm-1,[23] demonstrating the existence of water molecules in trace amounts in the nanoparticles [24]. These water molecules may be caused by solvent residues or air humidity [23].

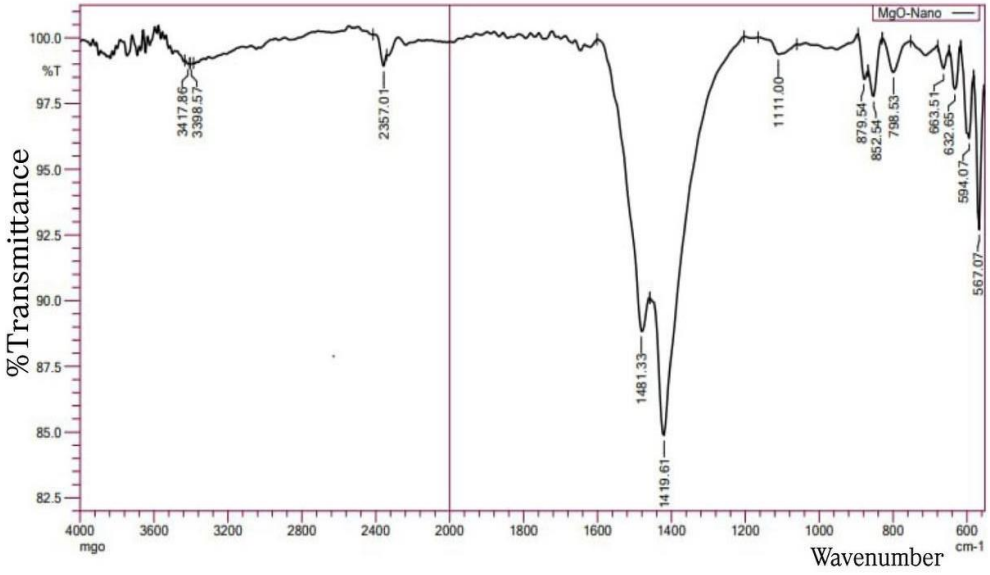

Figure 1: FT-IR spectrum of prepared MgO NPs.

3.2. Atomic force microscope (AFM)

Analysis of the 3D and 2D AFM images (Fig. 2) reveals that the particle surfaces were irregular, with agglomerated regions appearing as white peaks, a feature attributed to the measurement technique used [25]. These images also show the quantitative measurements of the prepared surface properties represented by the root mean square roughness (Rq) and the mean roughness (Ra), as well as the maximum height from peak to valley (Rt) [26]. The measured Ra, Rq, and Rt were 1.180, 1.608, and 5.91 nm, respectively. These values show that the particles are 3.23 nm in size and have a maximum thickness of 14 nm.

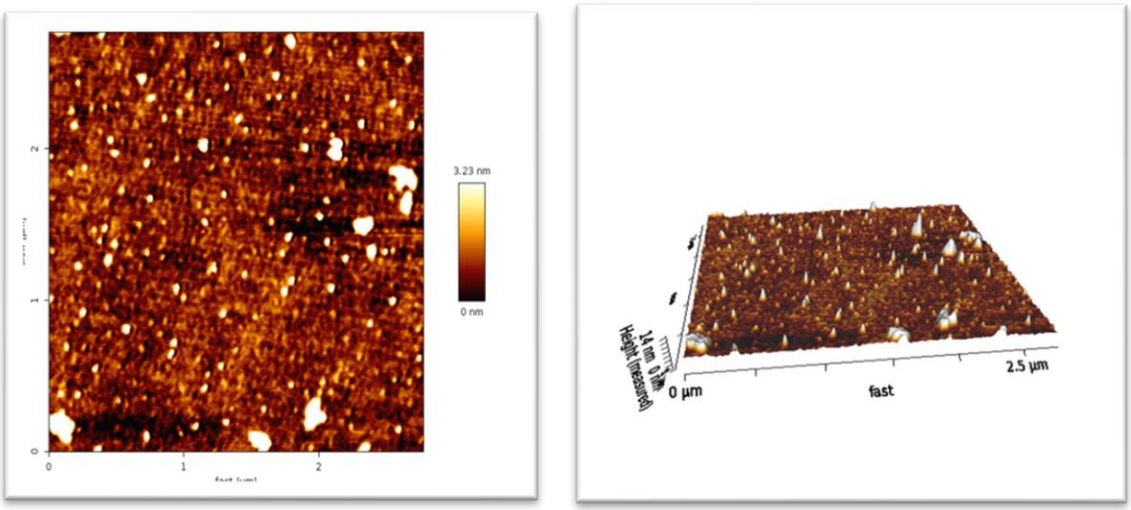

Figure 2: AFM image of the prepared MgO NPs.

3.3. SEM microscopy

Images captured by scanning electron microscope of MgO NPs reveal a strong and evident attraction between the prepared particles [27]. The particles have a large surface area because of their morphology, which is in the form of structures resembling nanosheets with flower-like nanostructures scattered throughout. The particle morphology was altered by the preparation technique, which is explained by the size and surface energy. [28]. Also, it was noted that the diameters of the particles range from 30 to 40 nm, as shown in Figure 3.

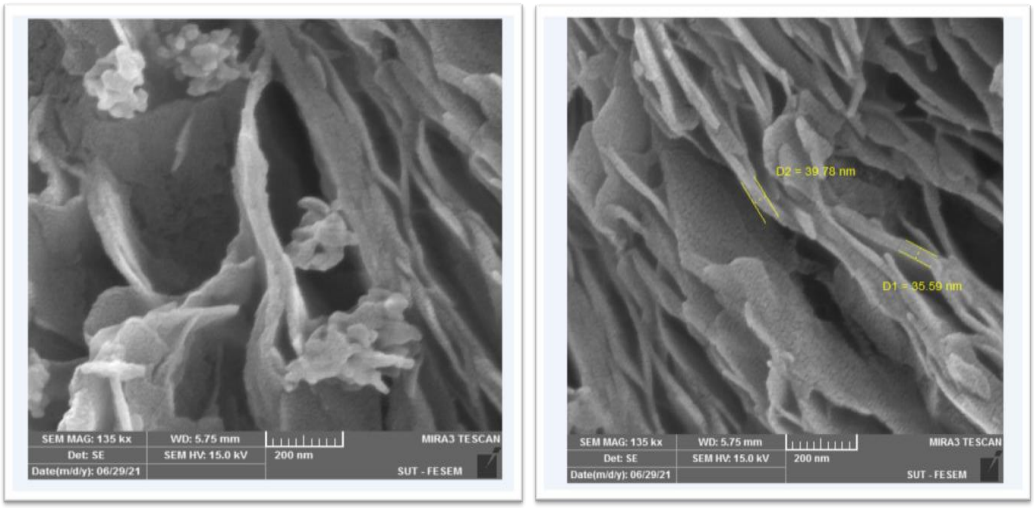

Figure 3: SEM photographs of prepared MgO NPs at 200 nm and 135kx magnification.

3.4. XRD spectroscopy

Figure 4 shows the X-ray diffraction (XRD) pattern of the resulting magnesium oxide nanoparticles. The 2θ-corresponding diffraction peaks were: 38.02, 42.82, 62.03,74.30, and 78.74, which correspond to the crystalline indices (1 1 1), (2 0 0), (22 0), (311) and (2 2 2) respectively, which reveal the formation of a polycrystalline [4,11]. This corresponds to JCPDS Card No. (89-4248), confirming the crystalline nature of the synthesized nanoparticles [3,11]. Using the Debye-Scherrer equation [22], the average crystallite size was determined to be approximately 30 nm. The following equation is the Scherer formula utilized to determine the crystalline particles:

$$D = (0.89\ \lambda)/(\beta \cos\theta) \quad (1)$$

Where β = width at half maximum peak (FWHM); D = particle size; and λ = the wavelength of x-rays [11].

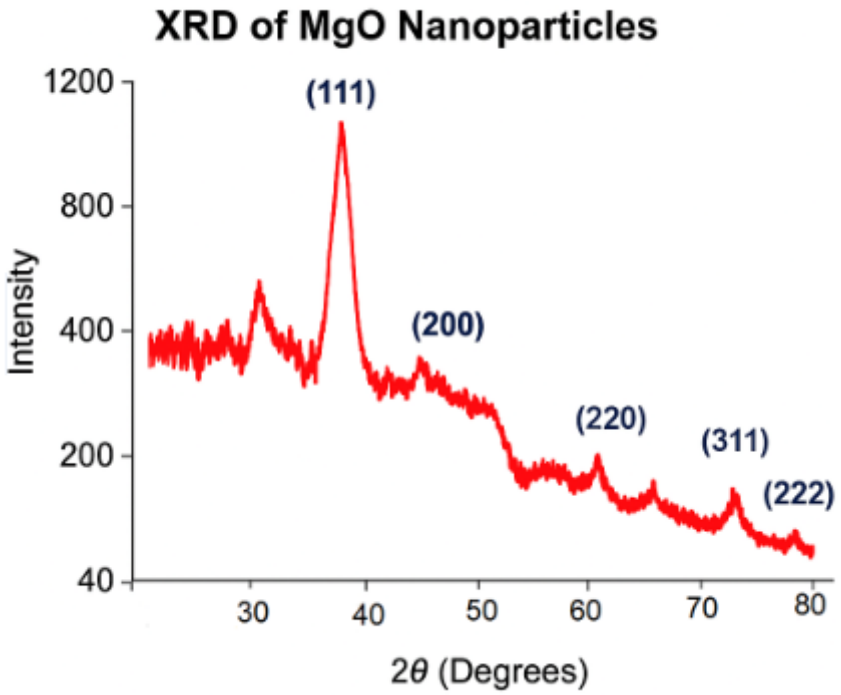

Figure 4: XRD spectrum of the prepared MgO NPs.

3.5. Surface area properties

The porosity and surface area of the adsorbent surface are among the factors that greatly affect the adsorption process [29]. Therefore, the Langmuir, Brunauer-Emmett-Teller (BET), and Barrett-Joyner-Halenda (BJH) techniques were used in this study [30]. Figure 5 illustrates the nitrogen adsorption-desorption isotherm on the surface of MgO NPs, used to determine their surface area based on monolayer nitrogen coverage [31]. At all pressures, the adsorption increases and reaches a constant amount at a pressure of 0.89, which reaches equilibrium [20]. Type II adsorption isotherms, which show multiple layers of adsorption, are followed by this phenomenon. Across all studied pressures, it was observed that decreasing the applied pressure resulted in reduced gas evacuation. This kind of isotherm is typical of materials with plate-like shapes and flexible pores, as well as of particles that aggregate [27].

It can be seen from Figure 6 that the Langmuir isotherm of nitrogen gas on the surface of MgO NPs is used to find out the surface area of the nanoparticles when covered with a single layer of nitrogen gas. The quantity of gas that has been adsorbed gradually decreases until it reaches a pressure of 84.785 (p / kPa), at which point it reaches a constant amount. It is observed that the adsorption of gas molecules increases with increasing pressure applied to the value of 46.989 (p / kPa) [32].

The t-plot is a method for determining the surface area of the material and for small sizes, or porosity. Figure 7 shows that when the pore size decreases, the value of t (plot) increases. Additionally, it observes that following pore filling, the t (plot) chart departs from the linear system. The prepared particles were found to have a surface area of 48.45 m^2 g^{-1} and a surface volume of 0.00823 cm^3 g^{-1} [29].

The BET diagram of nitrogen gas adsorption on a surface up to its maximum value of 0.064539 at a pressure of 0.453 (P / P0), as shown in Figure 8, illustrates how the nitrogen gas molecules expand with increasing applied pressure. Thus, it follows that MgONP nanoparticles may absorb nitrogen gas at all pressures investigated [31].

Figure 9 shows the BJH pore size distribution derived from nitrogen adsorption on MgO NPs, which exhibit a surface area of 34.715 m^2 g^{-1} and an average pore size of 1.2126 nm. These characteristics, high surface area and small pore size—indicate high adsorption capacity and effectiveness [33]. The main reason for the discrepancy in interpretations between the BET diagram and the t-plot containing the BJH of the particles under study is Micro pares surfaces are inappropriate for the BJH model.

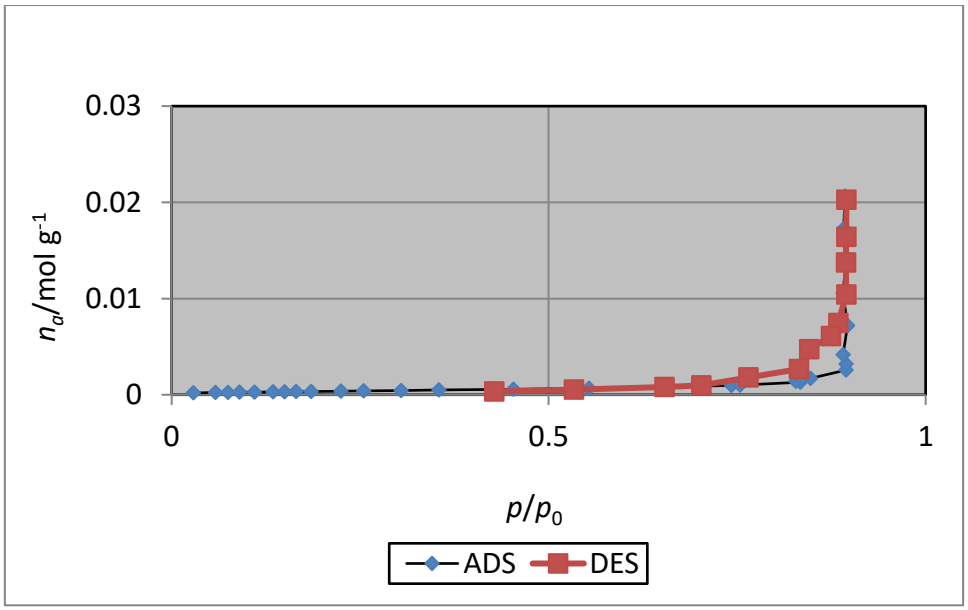

Figure 5: Adsorption-desorption isotherm of prepared MgO NPs.

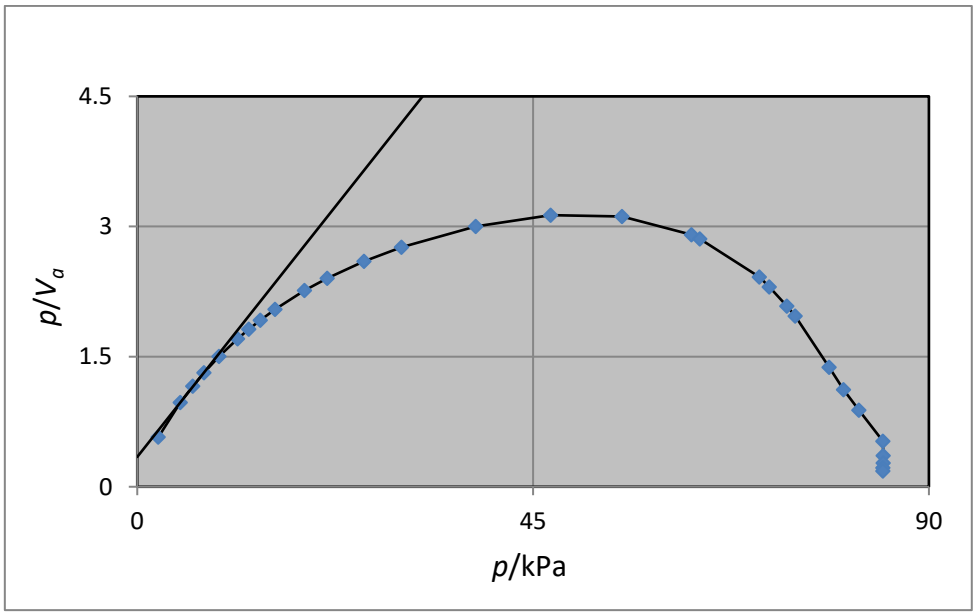

Figure 6: Langmuir –a plot of prepared MgO NPs.

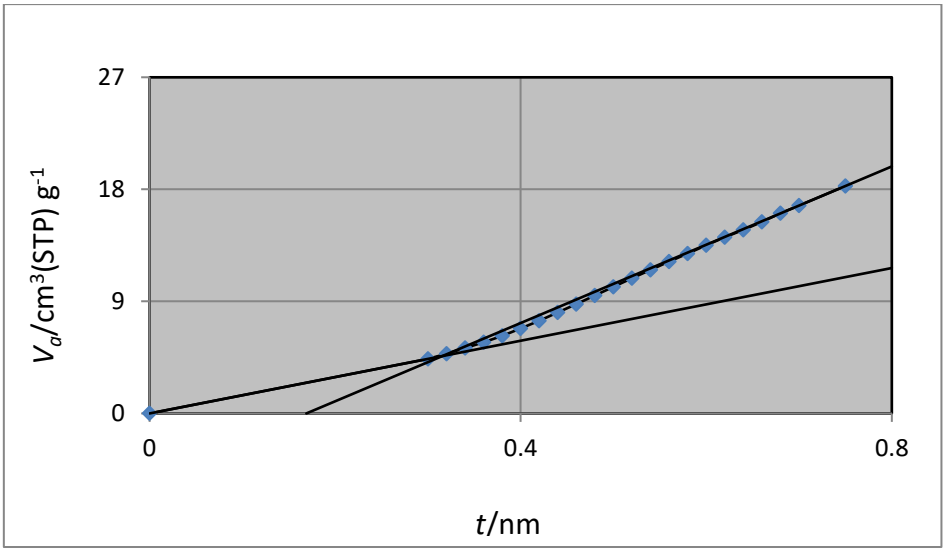

Figure 7: T-plot of prepared MgO NPs.

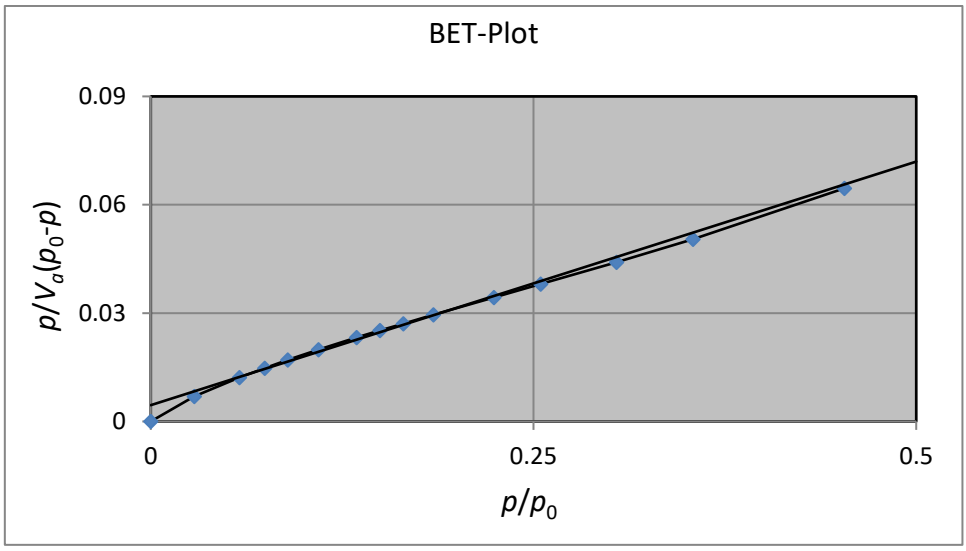

Figure 8: BET plot of adsorption of prepared MgO NPs.

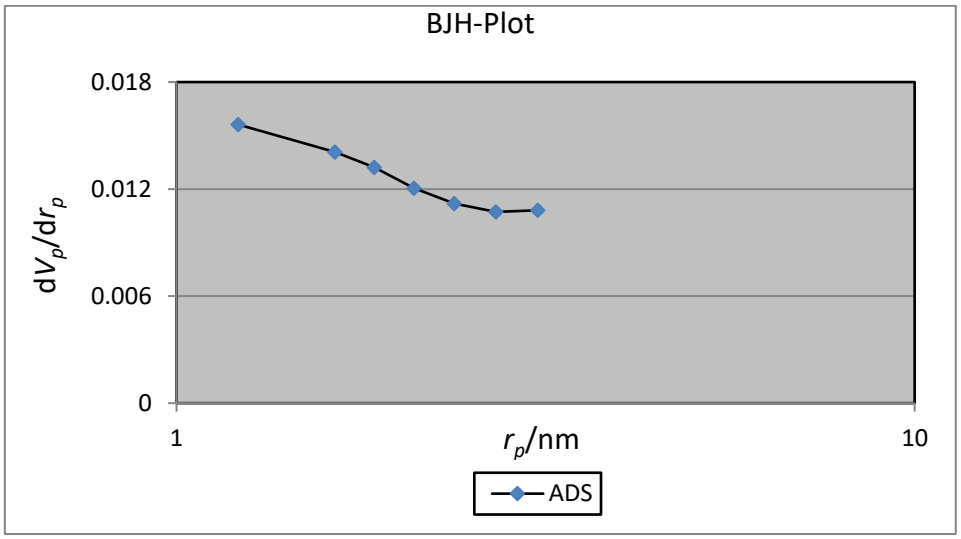

Figure 9: BJH plot of adsorption of prepared MgO NPs.

Conclusion

MgO NPs were successfully synthesized by the co-precipitation method. The nanoparticles were characterized by FTIR, SEM, AFM, and X- XRD. This synthesis method produced highly pure nanoparticles exhibiting nanosheet-like structures interspersed with flower-like nanostructures in their morphology. The average size of the prepared particles as determined by SEM, AFM, XRD, and BET chart ranges between 30 and 40 nm. In addition, it was observed that 31.227 m^2 g^{-1} is the specific area based on BET absorption. According to the BJH model, the average pore diameter is 1.21 nm, and the cumulative pore volume is 0.030311 cm^3 g^{-1}. One of the many uses for surface chemistry that can profit from its large surface area and small nanoparticle size is wastewater treatment. Magnesium oxide particles can also be used after being mixed with any other metal or organic compound, and their surface area, nanosize, and pore diameter changes are measured.

References

[1] K. S. Mohan, Z. T. Omran, T. A. S. K. Salman, and I. H. Al-Masoodyb, "Evaluation of Combinations between Menthe Extract, Zinc Nano Oxide and Phenol Compound on Antifungal," *Institute of Physics Conference. Series: Earth and environmental science*, vol. 1215, no. 1, 2023, doi: 10.1088/1755-1315/1215/1/012064.

[2] R. J. I. Shaik, A. Vohra, R. Devkar, "Synthesis, Characterization, Structural Features and Cytotoxicity of Innovative zinc(II) Complex Derived from ONS-Donor Thio-Schiff Base of Acyl Pyrazolone" *European journal of chemistry*, vol. 10, no. 2, pp. 131–138, 2019, doi: 10.5155/eurjchem.12.1.86.

[3] S. Narendhran, M. Manikandan, and P. Baby Shakila, "Antibacterial, antioxidant properties of Solanum trilobatum and sodium hydroxide-mediated magnesium oxide nanoparticles: A green chemistry approach," *Bulletin of Materials Science*, vol. 42, no. 3, 2019, doi: 10.1007/s12034-019-1811-7.

[4] A. Amir, M. Faisal, M. A. Hussain, E. Ul Haq, K. Raza, and Z. ur Rehman, "A facile synthesis of nano-magnesia by ultrasonication assisted co-precipitation method for antibacterial activity," *International Conference on Modern Technologies in Mechanical & Materials Engineering*, vol. 398, p. 01037, 2024, doi: 10.1051/matecconf/202439801037.

[5] I. Ben Amor, H. Hemmami, S. E. Laouini, H. Ben Temam, H. Zaoui, and A. Barhoum, "Biosynthesis MgO and ZnO nanoparticles using chitosan extracted from Pimelia Payraudi Latreille for antibacterial applications," *World journal of microbiology & biotechnology*, vol. 39, no. 1, 2023, doi: 10.1007/s11274-022-03464-5.

[6] M. Ramezani Farani, M. Farsadrooh, I. Zare, A. Gholami, and O. Akhavan, "Green Synthesis of Magnesium Oxide Nanoparticles and Nanocomposites for Photocatalytic Antimicrobial, Antibiofilm and Antifungal Applications," *Catalysts*, vol. 13, no. 4, 2023, doi: 10.3390/catal13040642.

[7] H. Kwang Benno Park *et al.*, "Optimization and modelling of magnesium oxide (MgO) photocatalytic degradation of binary dyes using response surface methodology," *Science Reports*, vol. 14, no. 1, pp. 1–13, 2024, doi: 10.1038/s41598-024-56797-6.

[8] N. A. A. Aboud, B. E. Jasim, and A. M. Rheima, "Adsorption study of phosphate ions pollution in aqueous solutions using microwave synthesized magnesium oxide nanoparticles," *Digest Journal of Nanomaterials and Biostructures*, vol. 16, no. 3, pp. 801–807, 2021, doi: 10.15251/djnb.2021.163.801.

[9] R. Ali, Z. J. Shanan, G. M. Saleh, and Q. Abass, "Green synthesis and the study of some physical properties of MgO nanoparticles and their antibacterial activity," *Iraqi Journal of Science,* vol. 61, no. 2, pp. 266–276, 2020, doi: 10.24996/ijs.2020.61.2.9.

[10] H. S. Al-Rikabi, M. H. Al-Timimi, and I. K. Abd, "A review of (MgO) thin films, preparation and applications," *American Institute of Physics*, vol. 2834, no. 1, 2023, doi: 10.1063/5.0176417.

[11] M. A. Ammulu, K. Vinay Viswanath, A. K. Giduturi, P. K. Vemuri, U. Mangamuri, and S. Poda, "Phytoassisted synthesis of magnesium oxide nanoparticles from Pterocarpus marsupium rox.b heartwood extract and its biomedical applications," *Journal of Genetic Engineering and Biotechnology*, vol. 19, no. 1, p. 21, 2021, doi: 10.1186/s43141-021-00119-0.

[12] A. Almontasser, A. Parveen, and A. Azam, "Synthesis, Characterization and antibacterial activity of Magnesium Oxide (MgO) nanoparticles.," *IOP Conference Series: Materials Science and Engineering*, vol. 577, no. 1, 2019, doi: 10.1088/1757-899X/577/1/012051.

[13] E. M. Sulaiman, F. A. H. Mutlak, and U. M. Nayef, "High-performance photodetector of Au–MgO/PS nanostructure manufactured via pulsed laser ablation technique," *Optical and Quantum Electronics*, vol. 54, no. 11, 2022, doi: 10.1007/s11082-022-04156-y.

[14] K. G. Manjunatha, B. E. K. Swamy, H. D. Madhuchandra, K. J. Gururaj, and K. A. Vishnumurthy, "Synthesis and characterization of MgO nanoparticle and their surfactant modified carbon paste electrode sensing for paracetamol," *Sensors International*, vol. 2, no. 8, p. 100127, 2021, doi: 10.1016/j.sintl.2021.100127.

[15] A. Bensouici, N. Baali, R. Bouloudenine, and G. Speranza, "Decoration of Reduced Graphene Oxide with Magnesium Oxide during Reflux Reaction and Assessment of Its Antioxidant Properties," *C — Journal of Carbon Research*, vol. 8, no. 4, 2022, doi: 10.3390/c8040049.

[16] M. Mylarappa, N. Raghavendra, B. S. Surendra, K. N. Shravana Kumar, and S. Kantharjau, "Electrochemical, photocatalytic and sensor studies of clay/MgO nanoparticles," *Applied Surface Science Advances*, vol. 10, no. October 2021, p. 100268, 2022, doi: 10.1016/j.apsadv.2022.100268.

[17] T. Naseem and T. Durrani, "The role of some important metal oxide nanoparticles for wastewater and antibacterial applications: A review," *Environmental Chemistry and Ecotoxicology*, vol. 3, pp. 59–75, 2021, doi: 10.1016/j.enceco.2020.12.001.

[18] B. B. Hasan, T. A. Salman, and A. K. Ayal, "Enhancing Electrochemical Cells Performance with Modified Ionic Liquids and Deep Eutectic Solvents using Titanium Dioxide Nanoelectrodes-Graphite," *Iraqi Journal of Science*, vol. 65, no. 10, pp. 5406–5415, 2024, doi: 10.24996/ijs.2024.65.10.6.

[19] A. A. Jasim, W. A. Jasim, and J. M. S. Jamur, "HPLC Method for the Determination of Some Antibiotic Residues in Different Hospitals Wastewater in Baghdad City, Iraq," *Chemistry and chemical technonolgy*, vol. 67, no. 6, pp. 21–28, 2024, doi: 10.6060/ivkkt.20246706.7035.

[20] S. A. Jadoo and J. A. Naser, "Adsorption Optimization of Congo Red Dye onto Electrospun Nanofibers of Polyacrylonitrile functionalized with Fe3O4Nanoparticles," *Institute of Physics Conference Series: Materials Science and Engineering*, vol. 928, no. 5, 2020, doi: 10.1088/1757-899X/928/5/052024.

[21] G. Balakrishnan, R. Velavan, K. Mujasam Batoo, and E. H. Raslan, "Microstructure, optical and photocatalytic properties of MgO nanoparticles," *Results Results in Physics*, vol. 16, no. 11, 2019, p. 103013, 2020, doi: 10.1016/j.rinp.2020.103013.

[22] S. Parveen and I. Ikram, "Assessing Magnesium Oxide Nanoparticles (MgONPS) for Improving Growth and Related Parameters of Chilli Plant Varieties," *Indus Journal of Bioscience Researchvol*, vol. 3, no.1, pp. 255–264, 2025.

[23] I. A. Najem, F. Abd, and S. J. Edrees, "Structural Characterization of (Mg (1-x) pb x O) -NPs by Modified Pechini Method" *Engineering and Technology Journa*, vol. 40, no. 6, 2021, pp. 848–854, 2022.

[24] E. U. Ikhuoria, I. E. Uwidia, G. O. Otabor, and I. H. Ifijen, "Comparative Analysis of Magnesium Oxide Nanoparticles Biosynthesized from Rubber Seed Shell and Rubber Leaf Extracts," *Biomedical Materials & Devices*, vol. 2, no. 0123456789, pp. 1078–1088, 2023.

[25] A. A. Nemea and B. I. Al-abdaly, "Improving the Performance of Titanium Oxide Nanocomposites as NO 2 Gas Sensors for Optimum Sensitivity" *Iraqi Journal of Science*, vol. 65, no. 3, pp. 1200–1211, 2024, doi: 10.24996/ijs.2024.65.3.3.

[26] S. V. R. Venkatachalapathy and M. H. R. Murugesan, "Characterization of MgO thin film prepared by spray pyrolysis technique using perfume atomizer," *Journal of Materials Science: Materials in Electronics*, vol. 31, no. 0123456789, pp. 14838–14850, 2020.

[27] L. Todan, B. Adriana, R. Trus, and V. Surdu, "Comparative Study of MgO Nanopowders Prepared by Different Chemical Methods," *Gels*, vol. 9, no. 8, pp. 624–643, 2023.

[28] H. P. Kavitha, "Magnesium Oxide Nanoparticles: Effective Antilarvicidal and Antibacterial Agents," *ACS Omega*, vol.8, no. 6, pp. 5225–5233, 2023, doi: 10.1021/acsomega.2c01450.

[29] M. Gayathiri, T. Pulingam, K. T. Lee, and K. Sudesh, "Activated carbon from biomass waste precursors : Factors affecting production and adsorption mechanism," *Chemosphere*, vol. 294, no. 133764, 2022.

[30] F. Rafiee, H. H. Ardeshiri, A. Gholami, and H. Ghafuri, "Synthesis and characterization of new photocatalyst-based tin (IV) 5 , 10 , 15 , 20-tetrakis (4-benzhydryl benzoate) porphyrin immobilized on Fe 3 O 4 nanoparticles for removal of organic dye from wastewater" *Materials Science and Engineering B*, vol. 308, no. 7, p. 117574, 2024, doi: 10.1016/j.mseb.2024.117574.

[31] S. Fu and W. Han, "Accurate characterization of full pore size distribution of tight sandstones by low-temperature nitrogen gas adsorption and high-pressure mercury intrusion combination method," *Energy science and engineering*,vol. 9, no. 1, pp. 80–100, 2021, doi: 10.1002/ese3.817.

[32] R. S. Sahib and J. A. Naser, "Preparation, Characterization and Surface Area Properties of Manganese Oxide Nanoparticles," *Annals of the Romanian Society for Cell Biology*, vol. 25, no. 5, pp. 2962–2969, 2021.

[33] N. Choudhary *et al.*, "Application of Green Synthesized MMT / Ag Nanocomposite for Removal of Methylene Blue from Aqueous Solution," *Wate*r, vol. 13, no. 22, pp. 1–13, 2021.